ORIGINAL ARTICLE

On the effects of cutting-edge angle on high-feed turning of Inconel 718© superalloy

Francisco Javier Amigo[1] · Gorka Urbikain[1] · Luis Norberto López de Lacalle[1] · Pablo Fernández-Lucio[1] · Octavio Pereira[1] · Asier Fernández-Valdivielso[1]

Abstract

Machining processes on heat-resistant superalloys—i.e., turbine cases, rings, or shafts—are challenging tasks. The high-added value of such parts makes cycle times be longer than expected. Recently, high-feed turning technique has attracted the attention of practitioners due to its high material removal rate capability. PrimeTurning™ tool unifies the concepts of high-feed and multidirectional turning using multiple active cutting edges. It should be capable of reducing machine downtimes in that kind of parts. However, to avoid early tool replacement and rejects on high added value parts, a deeper knowledge on the high-feed turning process is necessary. Here, inserts specifically designed for high-feed turning in heat resistant Inconel 718© alloy were tested using three cutting-edge angles. The results showed that when chip thickness is more relevant, a cutting-edge angle of 30° reduces the likelihood of notches. Even if force components are high, surface roughness is improved and the risk of fractures is minimized, together with a high evacuation volume. On the other hand, increasing the cutting-edge angle (45° and 60°) without compensating the feed rate, tends to produce tool fractures due to chip overload. Besides, experimental tests showed that long tool-to-workpiece contact times, tend to shorten tool life, due to excessive heat accumulation and poor chip control.

Keywords High-feed · Turning · Superalloys · Cutting-edge angle

1 Introduction

The introduction of new tools and techniques for machining aerospace superalloys needs always a hard, in-depth, and test campaign which brings useful information. Basic processes and tools evolve together with the development of new multitasking machines, with superior capabilities. Among the latest innovative trends in turning, common objectives are increasing efficiency rates or decreasing tool change times. To reduce time costs and energy, longer-lasting inserts are designed for lower unit times. Different tools and inserts were developed specially for high-feed machining, from round inserts with variable angle or multiple radius inserts to wiper geometries and even to dynamic turning technologies with rotary tools allowing for multiple edges. For instance, Bushlya et al. [1] developed analytical models for various chip area parameters in turning with indexable round tools at different cutting conditions. However, round and multi-radius inserts can present chatter problems due to the length of the cutting edge involved in the cut [2]. With the aim of a good surface finish, wiper edges were also used in some cases. These are capable of joining together better surface roughness and higher feeds with respect to conventional inserts. Jiang and Wang [3] investigated through FE simulation the performance of different geometries of wiper tool edges. They concluded that wiper tools can reduce the temperature at the flank face compared to the conventional tool but, on the contrary, the temperature on the rake face increases due to the increased contact area. Besides, edges tend to create a curvature in the chip causing an early separation from the rake face, thus reducing wear. However, these types of edges also tend to increase machining forces as to create residual stresses close to the machined surface. Fujimaki et al. [4] proposed a method that extends the concept of the wiper tool to the turning of curved profile parts. To improve smoothness, a cutting-edge radius is selected close to the desired radius of curvature of the surface to

✉ Gorka Urbikain
gorka.urbikain@ehu.eus

[1] Centro de Fabricación Avanzada en Aeronautica (CFAA), University of the Basque Country, Bilbao, Spain

be machined. These authors obtained better machining efficiency rates, vibration stability, and smoother surfaces. Correia and Davim [5] compared the surface roughness between wiper and conventional cutting edges on carbon steel and found that at high-feed rates of 0.25 mm/rev the roughness is reduced—halved—when using the wiper edge.

The basic concept for high-feed turning is reducing the cutting-edge angle so that a greater length of the edge participates in the cut. In this way, the energy and heat created during cutting is moved away from the tip of the tool, local temperatures are not so damaging and so, the degradation rate (wear) of tool is reduced. Different investigations took into account the influence of the cutting-edge angle on forces, surface finish, or speed in conventional turning processes. Rahman et al. [6] experimented with variations of the side cutting edge angle (considering it as complementary to the rake angle) in Inconel 718 obtaining an improvement in insert life with increasing this angle (therefore, insert life improved with decreasing rake angle). Saglam et. al [7] investigated the influence of the cutting-edge angle on steel parts using 4 different angles. They found important consequences on the shear forces and interface temperature. In addition, they stated that small angles relieved the pressure on the tip being advantageous for heavy or intermittent cuts. However, reducing cutting edge angle also leads to the rise of temperatures and to excessively thin chips that accelerate tool wear. Cascón et al. [8] proposed a force prediction model from CAM simulations along the machining path of non-symmetric parts. In order to mitigate the effects of intermittent hitting, the possibility of reducing cutting edge angle was explored. They observed that cutting forces decreased when decreasing this angle, a result supported in [7].

High-feed processes were first intended for roughing of steel and aluminum alloys, due to the increase in the cutting forces. Currently, new specific tools have been designed. Thanks to a greater robustness of the machine-tools and knowledge of materials, new-tech tools were specially developed for machining superalloys. However, allowable feeds are significantly lower than those used for the steels. For instance, Khan et al. [9] used 45° beveled inserts for high-feed turning of titanium alloy at various feed rates, achieving good roughness and tool life in PCD inserts.

Specifically, PrimeTurning™ process was developed to be able to perform multi-directional high feed machining, including facing operations in a single operation. For a conventional straight longitudinal turning, PrimeTurning™ provides a constant angle of 30° (Fig. 1, blue dots). However, in profiling operations (red dots in the downward inclined zones) Kr is variable. So, to achieve a constant chip thickness in downward trajectories, it is necessary to decrease feed rate. At angles close to 90°, feed is reduced to the half. In conventional turning, Kr is close to 90° in a straight cylindrical turning; so, using high-feed technique, it is possible to double the feed while maintaining the same chip thickness and, in theory, maintaining the same useful tool life. Due to the insert design, turning with upward profiles is only allowed for very slight slopes-below 30°. Otherwise, there is a risk of collisions and bad chip evacuation. If Kr is going to change during cutting, it is preferable to vary the feed rate to maintain control over the chip thickness. In this way, more complex applications such as dynamic turning require advanced—adaptable—software to continuously modify feed rate during cutting.

Pioneering works dealing with high feed inserts are found on relatively low hardness materials. Ráczi used type B insert in the machining of steel parts, obtaining good results for roughing, maintaining good stability, surface finish, and chip removal [10]. Krajčoviech et al. [11] investigated the

Fig. 1 Relationship between feed rate and cutting-edge angle for a given chip thickness
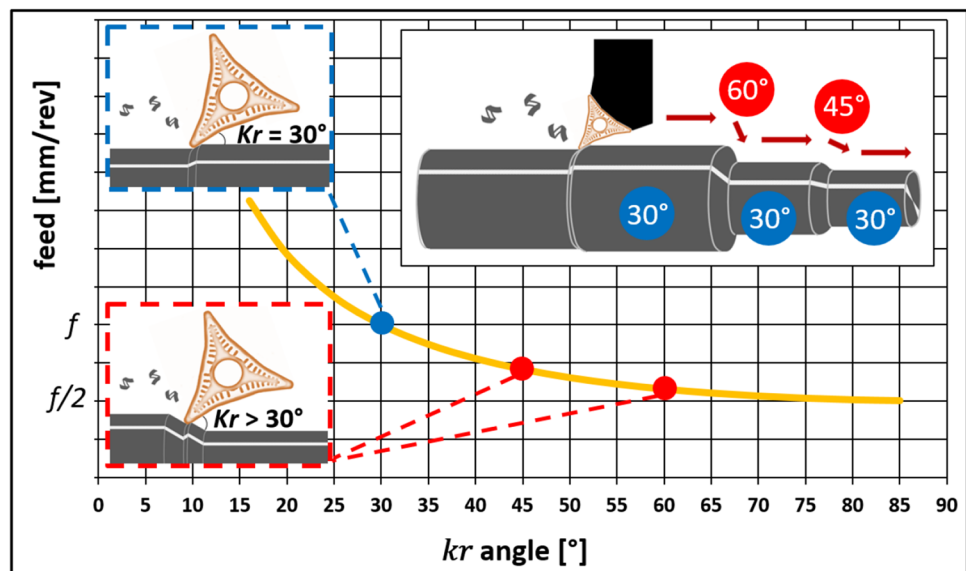
forces when machining carbon steel using the PrimeTurning™ process with type A insert. They obtained that the depth of cut has a significant effect on cutting forces. Then, Amigo et al. [12] investigated forces and surface roughness when turning superalloys. Specifically, they developed force prediction models and compared cutting tool performance under different materials (steels and superalloys) and coolant conditions (emulsion-based conventional and cryogenic CO). Karpuschewski et al. [13] tested different feed speeds to obtain cutting coefficients when using a rhombic insert. Interesting relationships were found between feed speeds and depth of cut affecting those coefficients.

In some aircraft engine components, the percentage of turning operations (in time or in percentage of removed volume) in relation to the total number of machining operations is high. This is the case of shafts, discscata, rings, or casings. In these types of parts, high-feed turning can reduce machining times, increasing productivity and maintaining the quality of parts with high-added value. Gómez-Escudero et al. [14] used high feed turning and PrimeTurning™ tools in the turning operations for the manufacture of a 0.92 m diameter AISI XM-12 stainless steel test aircraft casing. High-feed tools showed high roughing qualities when using feeds up to 1.75 mm/rev with a very low position angle of 18.5°. However, high cutting forces are also generated (> 5000 N), so needing stiffer clamping systems.

When inserts are inclined, chip thickness can be controlled by varying the feed rate. This is the basis for instance in plunge or axial milling process where Kr is reduced so that feed (feed per tooth, in milling) can be increased ($h_{max} = f \cdot \sin\kappa_r$). So, feeds f and Kr are inversely proportional. If chip thickness is to be kept at a stable size, an increase in Kr must be combined with a decrease in feed and vice versa. The greater durability of the insert due to the inclination of the cutting edge (reducing Kr) allows a margin to increase feed rate. Thus, chip thickness can be adapted to the operation type. Zhang et al. [15] performed finite element simulations to investigate chip characteristics and their variation as a function of various parameters, including feed rate. They obtained that the maximum chip thickness almost equals feed, and that the increase in feed produces a greater degree of chip segmentation also increasing the height of chip roughness, as well as the space between chips. Different authors investigated the difficulty of profiling and contouring operations. Reddy et al. [16] performed tests on complex profile aluminum parts, with variable concave and convex contours with the aim of developing variable force models. They concluded that contouring operations were significantly improved when reducing lead angle.

Obtaining and studying forces in turning is an important milestone as they are often related to tool wear, surface integrity, and chatter processes. Choudhury and Kishore [17] developed a mathematical regression model for flank wear

prediction. To do so, they monitored cutting force data and considered the relationship between the force components. The regression model was validated with experimental tests. Oraby and Hayhurst [18] also used the relationships between cutting force components to create a wear model using nonlinear regression techniques. The results were successfully validated with experimental results and with predictions of an extended Taylor model. Zhang et al. [19] conducted a study of various turning operations such as straight turning, contour turning, taper turning, and facing to obtain a mechanistic model of the cutting forces in order to predict the cutting forces by differentiating each operation. Cui et al. [20] studied the tribological characteristics when machining difficult-to-cut alloys. These authors proposed a systematic approach based on force, tool wear, chip, and surface integrity in titanium alloy and nickel alloy machining.

Inconel 718 superalloy is cataloged as a hard and low machinability material, producing greater damage to inserts than other superalloys. Therefore, different studies were focused on increasing tool life and analyzing how machining affects surface quality. Toubhans et al. [21] investigated the machinability of Inconel 718 and how work hardening affects accuracy due to residual stresses. They developed a mechanistic force model including tool wear estimation. Residual stresses were analyzed according wear level. Proper chip breaking efficiently removes heat from the process and has a positive effect on tool life and stability of machining operations, but variations in position angle and feed rate affect chip breaking. Ceramic inserts do not have a chip breaker on the chipping face and this affects their service life. Sugihara et al. [22] analyzed the behavior of CBN inserts in high-speed turning of Inconel 718. They proved that tool failure was mainly caused by crater and flank wear induced by diffusion effect due to high temperatures. To avoid this problem, CBN inserts were modified with micro grooves on the flank face. Cutting edge chipping was reduced, and so, tool life was improved. Following the same trend, Fernández-Lucio et al. [23] carried out a substrate characterization of PCD inserts to generate different chip breakers by laser texturing and apply them to improve the machining of aeronautical parts with Ti6Al4V alloys. These inserts do not have chip breakers due to the extreme manufacturing conditions, so texturing parallel to the cutting edge proved to be the best option to fragment the chip. Long and Huang [24] carried out an analytical development of how crater wear; in combination with flank wear, influences cutting forces, an aspect that had been disregarded. They proposed a slip line-based force modeling approach to capture the shear mechanism under the effects of flank and crater wear. Grechishnikov et al. [25] presented a technique for predicting some microscopic irregularities in turning of intricately shaped parts. Panda et al. [26] used principal component analysis (PCA) for the optimization of surface

quality characteristics (Ra, Rz, and Rt) during turning operation on EN-31 steel. The optimal process parameters for surface roughness i.e. Ra and Rz are the depth of cut 0.5 mm, the cutting speed 140 m/min, and the feed 0.04 mm/rev.

Some other works are focused on improving surface quality. To do so, some of them, use alternative cooling techniques, such as MQL or cryogenic cooling. Pereira et al. [27] used CO2-CryoMQL lubrication, where oil flow rates are drastically reduced, in milling Inconel 718 and obtained a tool life reduction of only 6.5% compared to oil emulsion. Behera et al. [28] performed a comparison between high-pressure, cryogenic, MQL, and nanofluid lubrication on Inconel 718. Cryogenic cooling improved surface integrity and tool wear. Krolczyk et al. [29] carried out a literature review on ecological advances in the machining of difficult-to-cut materials. In this study, cryogenic cooling and MQL/MQCL are highlighted as the most promising. In high-pressure cooling, the reuse cycle and the design of the ducts must be studied. There is a general agreement that MQL based on nanoparticles and MQCL based on EP/AW additives are very important methods, but their life cycle and inhalation health risk should be analyzed. Biodegradable oils improve surface roughness and their hybrid use with nanofluids in MQL can improve efficiency, but their toxicity to humans needs to be studied. Cryogenic cooling is also very advantageous in processes, but its high implementation cost is a drawback for industrial use. Dry machining is very eco-sustainable but very difficult to apply to heat-resistant materials, and cost–benefit studies of coatings must be carried out. In the same way, Khanna et al. [30] reported the evolution of cryogenic cooling systems as a sustainable technology for machining different materials. The results show a wide range of possibilities but hybridization between different techniques such as cryogenic cooling and minimum quantity lubrication, electrostatic MQL, and nanofluid-based MQL tends to be considered beneficial for difficult-to-cut materials. Previously, Devillez et al. [31] had investigated the dry cutting of Inconel 718, using coated carbide tools under semi-finishing conditions. They optimized a cutting speed of 60 m/min for which the surface quality is acceptable, without major alterations in the microstructure. This cutting condition limits the residual stresses and the affected depths and tensile stresses. This study demonstrates the restricted use of dry machining of heat-resistant materials. Ibrahim et al. [32] evaluated the effect of MQL and NFMQL on cutting force, surface roughness, flank wear, and cutting temperature during hard turning of AISI D3 steel. The use of zinc oxide as a nanofluid seemed to be very advantageous. Specifically, roughness can be improved between 4 and 13%. Maruda et al. [33] evaluated surface integrity during turning of AISI 1045 under dry conditions, using MQCL method and using MQCL method with extreme pressure/anti-wear additive (EP/AW). The lowest Sa and Sz surface roughness values were reached in MQCL + EP/AW machining process, from 12 to 70% in comparison to machining without cutting fluids and from 6 to 29%, comparing to MQCL turning. Gupta et al. [34] studied the machining of 2205 duplex steel by applying MQL on the flank face, rake face, and both faces. They found that the surface roughness and wear values were reduced to a greater extent by using MQL on both faces. Similar results were obtained by Krolczyk et al. [35]. They carried out an experimental study on roughness in duplex steel turning, under dry cutting conditions and MQL, for the benefit of sustainable cooling and to avoid the contaminating effects of machining fluids. Significantly better results were obtained with MQL due to its good cooling and lubrication capacity, concluding that this technique improves the machining of difficult-to-cut materials where dry cutting does not evacuate the heat generated in the cutting zone. Amigo et al. recently gave some key results for improving high-feed turning technique when superalloys are machined. Particularly in [12] they presented a force model and in [36] they presented some guidelines for chipbreaker design.

In this study, a set of experimental turning tests on Inconel 718 were carried out to characterize tool behavior in terms of cutting-edge angle. Section 2 develops the experimental procedure followed to measure cutting forces and surface roughness. Section 3 analyzes the results from the wear tests. Finally, some conclusions are drawn in Section 4.

2 Experimental setup

2.1 Materials and equipment

Cutting tests were done in a Mazak Integrex i200. Cutting tools are PrimeTurning™ type A inserts (Fig. 1): ISO code CP-A1108-L5, grade GC1115, HC substrate and PVD coating (TiAlN + TiAlN), with grain size below 1 μm, (HRc = 80 and fracture toughness = 8.8 MPam$^{1/2}$), with inscribed circle diameter iD = 11 mm de dimensions and non-standard shape, with three edges, nose radius $r\varepsilon = 0.794$ mm; insert angle = 35°, side cutting edge angle Kr = 30° and rake angle $\gamma = 0°$.

On the other hand, a bar of Inconel 718 (UNS N07718 / W.Nr. 2.4668) is used. This material belongs to the Nickel–Chromium group and is widely used not only in gas turbines but also in nuclear reactors, pumps, etc. The work material was supplied in aged state: the material is hardened by precipitation of secondary phases into the metal matrix. Table 1 shows the main properties.

A Kistler 9257B dynamometer is used for monitoring turning forces while surface roughness is evaluated using a Taylor Hobson® Surtronic Duo portable roughness meter. As cutting fluid, Quaker Houghton Hocut®4260

oil and water emulsion is selected, with a concentration of 10% and a flow rate of 6 l/min.

2.2 Clamping and reference systems

The dynamometer is held by a Capto 6 adapter so that it can be attached to the machine head. This head is very voluminous, so the horizontal position is limited by the tailstock (Fig. 2). Therefore, the head must be positioned vertically forcing the cutting edge to attack the part laterally, from behind the bar, on the negative side of the Y axis of the machine. In this way, it is necessary to rotate the tool 90° inside the jaw of the dynamometer so that tool's rake face is directed with the rotation of the bar. So, a transformation between Z and Y axes is necessary.

For $\kappa r = 30°$, the position of the dynamometer remains parallel to the bar so that the whole cutting length can be used, as seen in Fig. 3a. Here, the machine reference system

Table 1 Composition and general properties of Inconel 718©

Chemical composition	Density [g/cm³]	Ultimate tensile strength [MPa]	Yield tensile strength [MPa]	Thermal conductivity [W/m•K]	Hardness HRc
52.5% Ni, 19% Cr, 17% Fe, 5% Nb, 3% Mo, 1% Co, 1% Ti, 0.6% Al, 0.35% Mn, 0.35% Si, 0.08% C, others	8.19	1.100 at 650 °C	1.100 (strain 0.2%)	11.4	45

Fig. 2 Positioning of head and tool
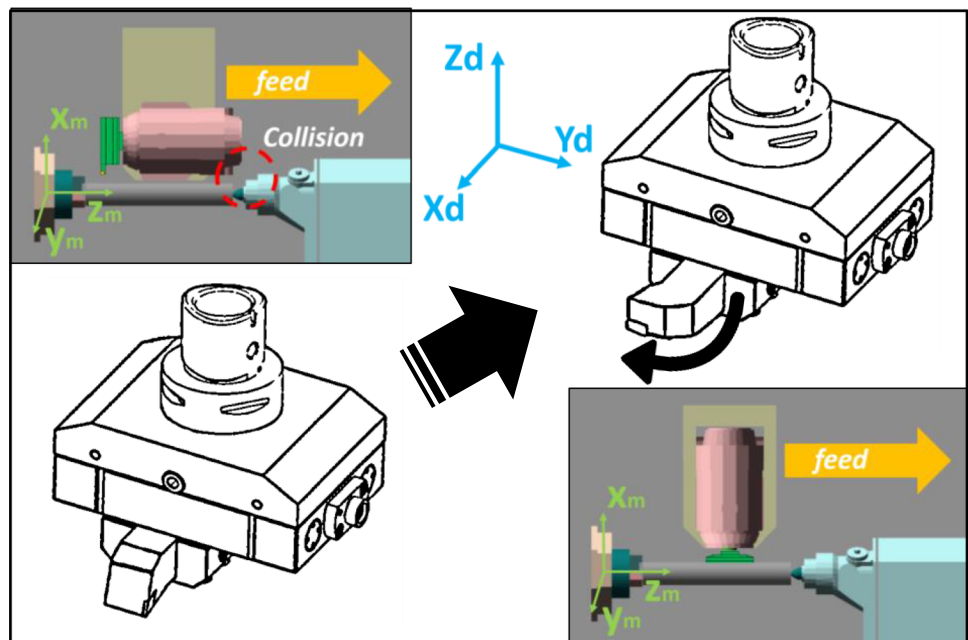
Fig. 3 Axes from Kistler for $\kappa r = 30°$ (**a**) and for $\kappa r > 30°$ (**b**)

(a)   (b)
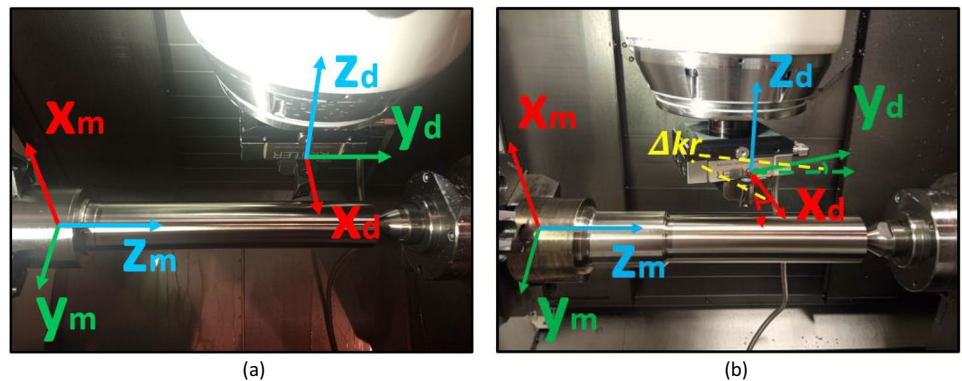
(X_m, Y_m, Z_m) and the Kistler reference system are represented. The orthogonal direction to the bar corresponds to the data track X_d, while the feed force is recorded in the track Y_d. The tangential component (parallel to V_c) is in the track Z_d. When cutting edge angle is increased till 45°–60°, the positioning of the dynamometer is not yet parallel to Z_m. Instead, it is further increased an angle Δ Kr (Fig. 3b).

To calculate force components in tool r-t-a system, a rotation of the reference system is required (see Fig. 4). To locate this system, we use a fixed position (from Kr = 30°) with respect to the horizontal surface of the part.

Therefore, to obtain the turning forces, tool axes must be transformed using Kr = 30°. In this way, the transformation between both systems can be derived from as follows:

$$\begin{pmatrix} Fr \\ Ft \\ Fa \end{pmatrix} = \begin{pmatrix} -cosKr & 0 & -sinKr \\ 0 & 1 & 0 \\ -sinKr & 0 & cosKr \end{pmatrix} \begin{pmatrix} Fxd \\ Fzd \\ Fyd \end{pmatrix} \quad (1)$$

Besides, do note the relationship between positions Y_d and Z_d, discussed above.

2.3 Design of cutting tests

Due to space limitations when it comes accessing the tool from *Y*-axis, it is necessary to use low diameter bars, with less than 70 mm. So, the amount of material that can be removed in such low diameters is limited. For this reason, we used two identical bars (specimens A and B) during the experimental tests. Table 2 shows the main cutting conditions. The design of the tests consists of longitudinal (straight) turning tests at 2 different cutting conditions that are repeated at 3 different cutting-edge angles—Kr = 30°, 45°, 60°—so that *Δ*Kr will be 0°, 15°, 30°, respectively.

In the tests in which *Δ*Kr = 0°, the cut is made in the total length of the bar. On the contrary, in the tests in which *Δ*Kr > 0° the rotation of the dynamometer prevents to take advantage of all the available bar length due to the impediment of the claws. The failure criterion is as usual VB = 0.3 mm (or the fracture of the flank face).

Figure 5 represents cutting geometry as a function of feed, depth of cut, and cutting-edge angle. It can be seen how, as Kr increases, chip thickness increases while width of cut decreases. This influences force component distribution and so, wear and tool life.

3 Results and discussion

Experimental tests under the two proposed cutting conditions and at three different position angles should provide useful information about the suitability of using decreasing

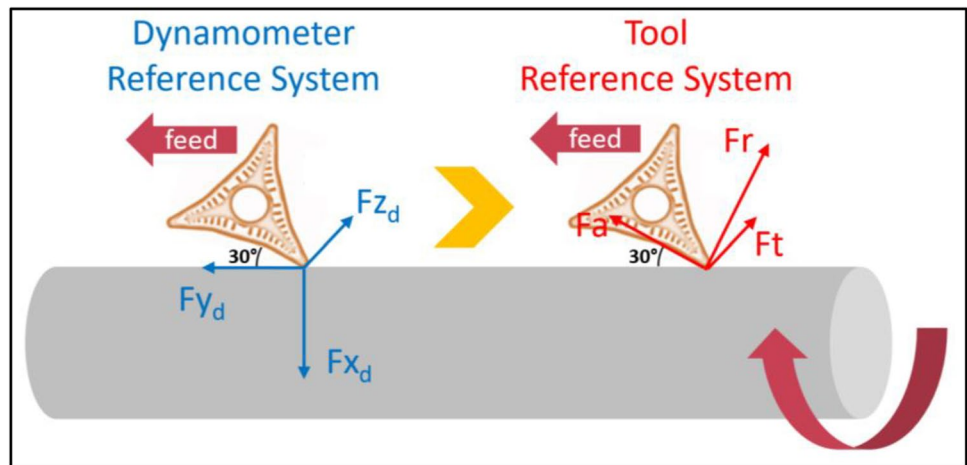**Fig. 4** Dynamometer and tool reference systems

Table 2 Cutting conditions

Cond	Kr [°]	ΔKr[°]	Vc [m/min]	f [mm/rev]	ap [mm]	MRR [cm³/min]	hm [mm]	L_BAR [mm]	D [mm]	Bar	N° Test
1	30	0	50	0.4	0.5	10	0.20	309.0–306.5	56.2–50.2	B	5
2			65	0.3	0.3	5.85	0.15	305.5–302.5	50.3–46.1	B	6
1	45	15	50	0.4	0.5	10	0.28	235.5–232.5	60.6–53.6	A	1
2			65	0.3	0.3	5.85	0.21	231.5–227.0	53.4–47.4	A	2
1	60	30	50	0.4	0.5	10	0.35	230.5	58.7–57.7	B	4
2			65	0.3	0.3	5.85	0.26	234.5–231.5	63.3–59.1	B	3

**Fig. 5** Chip thickness h_m, for different combinations of ap–Kr
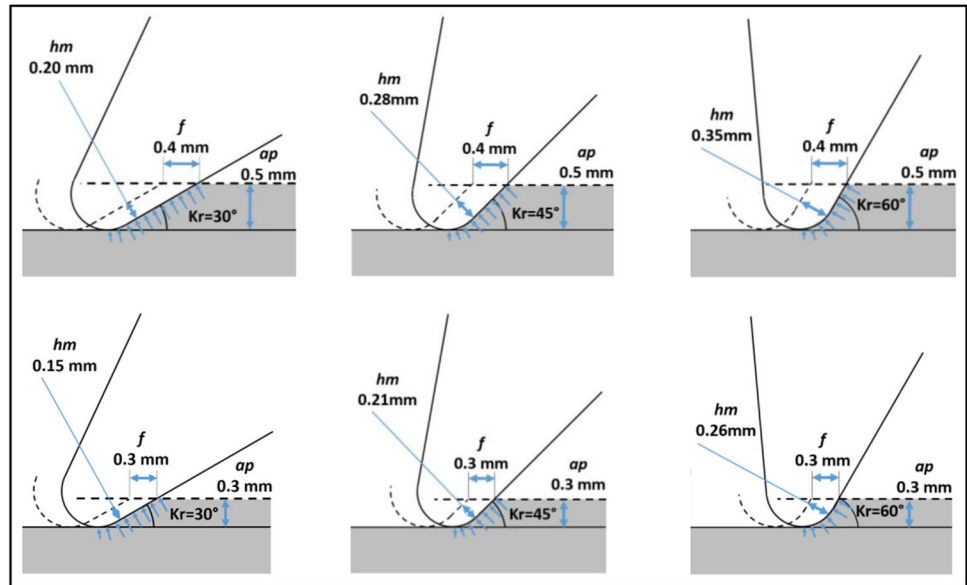
position angle depending on the conditions used. Comparison of the lifetime of the inserts is often a significant parameter, as well as the volume of material removed. On the other hand, machining forces provide useful information on the limits of the processes and can be an indication of the evolution of edge wear and its effect on the material to be machined. Surface roughness helps to explain the process of insert degradation and how variations in the insert, such as the position angle and improve surface finish.

3.1 Tool life

Figure 6 shows the evolution of flank wear under both conditions. Tests under condition 2 show a greater insert tool life than tests under condition 1. So, if in cutting condition 2, feed rate and depth of cut decrease with respect to condition 1, it can be stated that their simultaneous effect decreases tool life in a more important way than cutting speed.

On one hand, Kr = 60°, condition 1 suffers early edge breakage, while condition 2 exceeds 15 min of machining. In both cases, chip thicknesses are the highest values (see Table 2). So, the tool breakage is due to high feed combined with high depths of cut. On the other hand, see Kr = 30° and 45°, we get a progressive and controlled flank wear at both conditions. Chip thickness in this case was lower, more favorable. So, the decrease in the angle kappa improves tool life, since chip section becomes thinner.

To complete the picture, Table 3 is showed. For each cutting condition and Kr, the flank wear evolution is tracked every 4-min intervals, to normalize the samples. The corresponding instantaneous and final machining times (when reaching the maximum flank wear) and the average cutting interval time are also given. In all the tests, tools show a pronounced BUE—material adhesion—especially at the first machining stages. At the final stages, the crater wear is also observed. As this goes deeper into the insert, the BUE effect
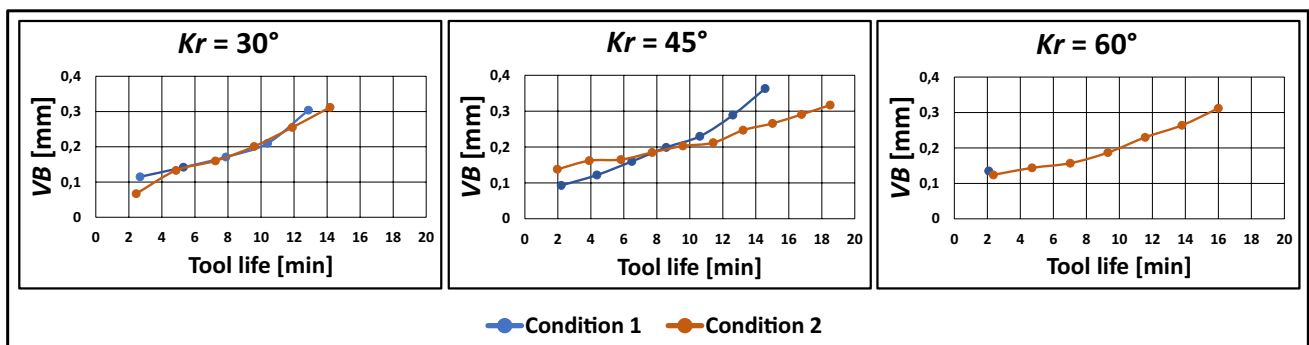
Fig. 6 Tool life (conditions 1 and 2)

Table 3 Tool wear evolution for the tested conditions

Cond.	Kr [°]	Cutting interval [min]						Tool life
		0	0<t<4	4<t<8	8<t<12	12<t<16	16<t<20	
1	30							12´46´´
	Time	0´00´´	2´41´´	7´53´´	10´24´´	12´52´´		$\bar{T}$=2´34´´
2	30							13´42´´
	Time	0´00´´	2´27´´	7´14´´	11´54´´	14´11´´		$\bar{T}$=2´22´´
1	45							12´54´´
	Time	0´00´´	2´12´´	6´29´´	10´37´´	14´34´´		$\bar{T}$=2´05´´
2	45							17´37´´
	Time	0´00´´	3´55´´	7´43´´	11´25´´	15´01´´	18´30´´	$\bar{T}$=1´51´´
1	60							2´05´´
	Time	0´00´´	2´05´´					$\bar{T}$=2´05´´
2	60							15´45´´
	Time	0´00´´	2´22´´	7´01´´	11´34´´	16´00´´		$\bar{T}$=2´17´´

tends to disappear. For Kr=30°, tool life in both cutting conditions is quite similar, barely increasing by 7.3% for condition 2. For Kr=45°, condition 1 suffers edge breakage during the last cutting interval, while tool life for condition 2 is considerably increased (up to 37%). For Kr=60°, condition 1 suffers early edge breakage, while condition 2 exceeds 15 min of machining. In both cases where tool breakage appears, chip thicknesses are the largest values, so the breakage is due to high feed and depth of cut values. However, this did not happen for Kr=30°, where the end of the test came due to flank wear. Chip thickness, in this case, was lower, more favorable.

Figure 7 shows (dashed blue line) the area of cutting conditions based on the recommendations by tool maker for a standard Kr=30°. The points selected in the tests are within the recommended area, thus using intermediate feed rates and low depths of cut.

When the position angle is increased to 45° and 60°, the operating area becomes narrower, decreasing the feed rates in order to maintain constant chip thicknesses. Because of this, the test points are increasingly placed towards the end of the recommended working area, as they have been performed without compensating the feed rate, and so the point

corresponding to condition 1 is outside the area when using Kr=60°, what explains the early fracture of the insert as it does not resist the stress of a chip thickness of 0.35 mm. When using Kr=45°, the point at condition 1 is just above the limit of the recommended area, with a chip thickness of 0.28 mm, which also leads to insert fracture (more later). Therefore, it can be stated that, for larger chips machined, the decrease in the kappa angle improves tool life, since chip section becomes thinner and the cutting edge must withstand lower stresses per unit length.

The application window is a manufacturer's recommendation for the whole group of heat-resistant superalloys. However, authors in [32] investigated chip breaking in machining of Inconel 718 with high-feed tools. They experimentally found the breaking limit under different conditions.

Figures 7 and 8 show these breakage limits in dashed yellow lines, while the chips obtained in the process can be seen in Table 4. As can be seen, the points at condition 1 are within the chip breaking zone and the chips obtained tend to break, at least in the initial stages. Subsequently, the chips become continuous, probably due to the deterioration of the chip breaker. Improvements in cooling should be implemented in the future to avoid early deterioration

Fig. 7 Cutting conditions recommended by the manufacturer and chip breaking limit
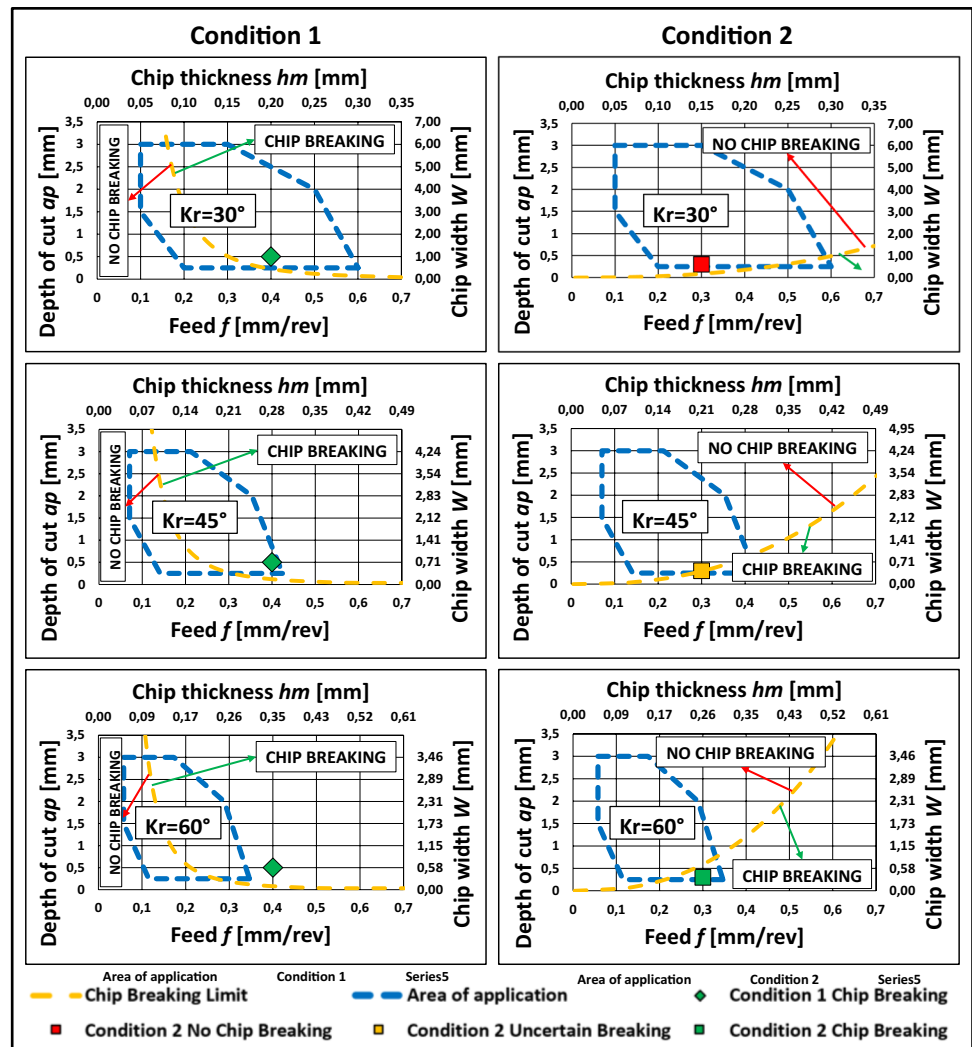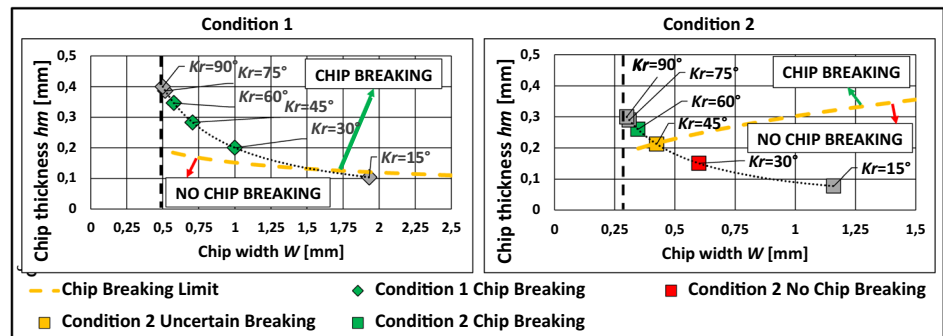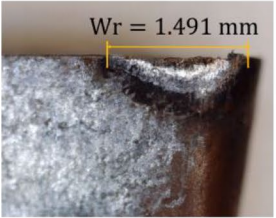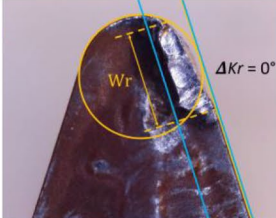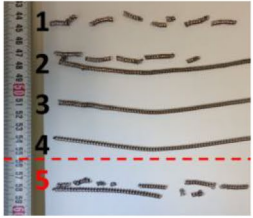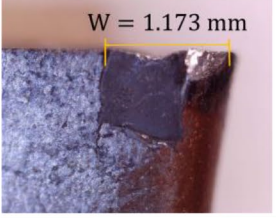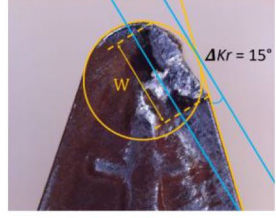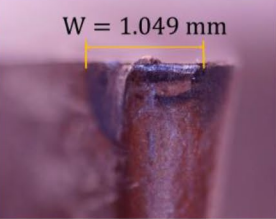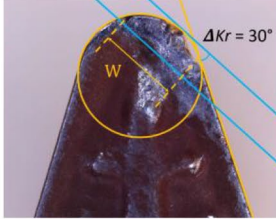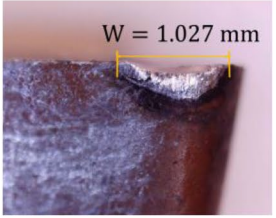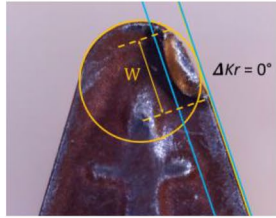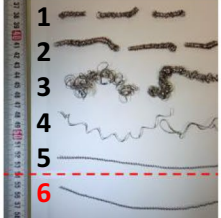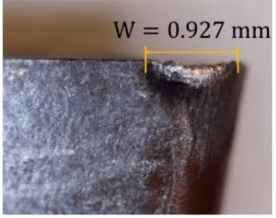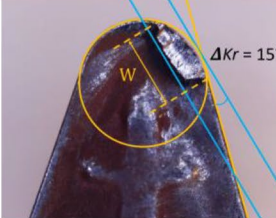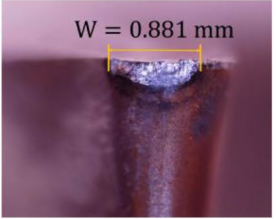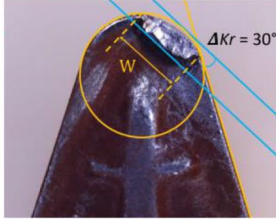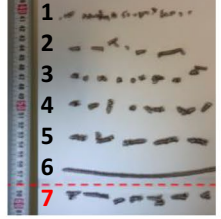

Fig. 8 Chip breaking limit

of the chip breaker. The point for condition 2 with Kr = 30° is outside the chip breaking zone and the chips obtained do not break correctly. The point for condition 2 with Kr = 45° is above the chip breaking limit and the chips obtained do not break properly either. Finally, the point for condition 2 with Kr = 60° is inside the chip breaking zone and the chips obtained break correctly in almost all stages.

Table 4 shows the flank faces in detail, with the measurements of wear width, as well as the rake face at the end of machining and the chips generated in the successive stages. As Kr increases, there is a smaller wear width. This allows to understand why, under condition 1, inserts tend to earlier failures with higher Kr: the lower the engaged length is, the more stress per unit length the insert must withstand.

Table 4 Wear features and chips

Kr [°]	Condition 1		
	Flank face	Rake face	Chips
30	Wr = 1.491 mm	ΔKr = 0°	
45	W = 1.173 mm	ΔKr = 15°	
60	W = 1.049 mm	ΔKr = 30°	

Kr [°]	Condition 2		
	Flank face	Rake face	Chips
30	W = 1.027 mm	ΔKr = 0°	
45	W = 0.927 mm	ΔKr = 15°	
60	W = 0.881 mm	ΔKr = 30°	

We do see that wear zones tend to move due to Kr. For Kr = 30°, wear width is maximum for both conditions studied, as cutting is composed by the round part of the cutting edge and the straight zone. But as Kr is increased with respect to tool flank, the wear width becomes narrower as cutting is only built from the round part. The least intuitive image comes from Kr = 60° (condition 1), since tool failure occurred early and wear direction is not well distinguished. In all the other cases, the effect of Kr is clearly appreciated. In general, the dominant wear mode is crater wear. This is especially true for condition 2. However, in these cases, chip breaker remains almost unaffected, while in condition 1 it clearly is affected. Edges from condition 2 show some notching at larger angles, but disappear for Kr = 30°. Smaller angles distribute forces more uniformly along the edge, reducing the tendency to notch wear.

3.2 Effect of cutting-edge angle

Condition 2 leads to a longer tool life than condition 1. On the other hand, the relationship between this tool life and Kr is not straightforward, the dependency is variable. As no parameter was fixed between both set of cutting conditions, a comparison of tool life would not be fair. However, considering both duration time and material removal rate, the total volume of removed material can be calculated to get an idea of tool performance (Fig. 9).

Condition 1 is very productive with both Kr = 30° and 45°; however, fractures in the inserts also occurred. The 60° test gave as result catastrophic failure at the beginning and the 45° test ended with another tool breakage, coinciding with the flank wear criterion, so the 30° test is the safest test and the most productive, evacuating 127.5 cm^3 of material. On the other hand, in condition 2 none of the inserts was broken: this is due to a smaller chip thickness; however, productivity was lower than in condition 1, evacuating 80 cm^3 of material in the 30° test, 103 cm^3 in the 45° test, and 92 cm^3 in the 60° test.
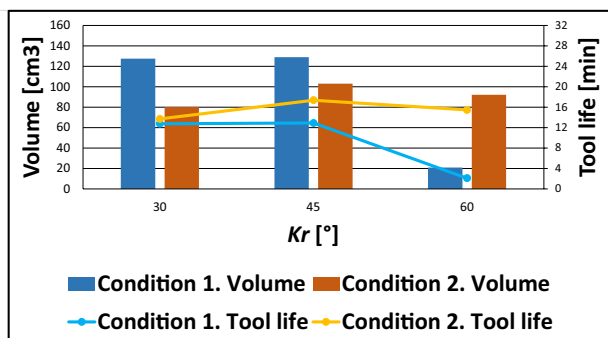
Fig. 9 Effect of side cutting-edge angle Kr on time and machined volume

The highest cutting performance in condition 2 was shown in 45° test, while the 30° test obtained an unexpectedly low performance. Table 3 shows the average times of the cutting intervals of each test. As can be seen, the average interval time in the 45° test is about 30 s lower than in the 30° and 60° tests. Inconel 718 is a very sensitive material to wear mechanism due to temperature. So, the shorter cutting times and the greater number of intervals and stops in this test favored less heating rates on the cutting edge, leading to a greater performance.

In summary, although machining times are longer in condition 2, these are jeopardized by tool degradation due to excessive cutting speed; this makes machining performance is better in condition 1. For low cutting speeds and high feed rates and depths of cut, machining performance is improved but the risk of fracture is high. In these cases, low Kr angles are advisable. For high cutting speeds and low feed rates and depths of cut, machining performance is reduced, but the risk of fracture disappears, so safety is increased and the use of low Kr is not so critical. However, the sensitivity to heat is greater, and so a good chip fracture and contact interval time are crucial. In this case, a suitable cooling is also advisable.

3.3 Force measurements

Figure 10 shows the radial, tangential, and axial components for all the tested geometries and cutting conditions. These are referred to the tool's reference system (*r, t, a*); thus, they were obtained from the measured forces using the transformation equation (Eq. 1). Forces are greater for condition 1, which increase the tendency to the commented edge breakage. As the tests evolve, the forces increase: Ft component is the most stable one, while Fr and Fa components are more variable over time. Fr forces are greatly affected by cutting-edge angle. For Kr = 30°, these forces increase much more, especially in the final phases. Specially, the increase of cutting forces is more evident in condition 1, where feed and depth of cut are greater. In condition 2, the evolution of the Fr component is more constant; however, when the angle is 60°, the force increases towards the end due to the local stress concentration in a narrower edge width. The reason for tool breakage (60°) in condition 1 is likely to be the same. It is noted that the greater the side cutting-edge angle, the smaller is the width of the worn edge.

- Condition 1 with Kr = 30°: Fr/Ft ratio varies from 0.58 at the beginning to 1.55 at the end. Condition 2: Fr/Ft ratio varies from 0.82 at the beginning to 1.71 at the end.
- Condition 1 with Kr = 45°: Fr/Ft ratio varies from 0.5 at the beginning to 1.08 at the end. Condition 2: Fr/Ft ratio varies from 0.63 at the beginning to 1.26 at the end.
- Condition 1 with Kr = 60°: Fr/Ft ratio is 0.43 at the beginning. Condition 2: Fr/Ft ratio varies from 0.56 at

Fig. 10 Cutting forces for different cutting-edge angles and cutting conditions
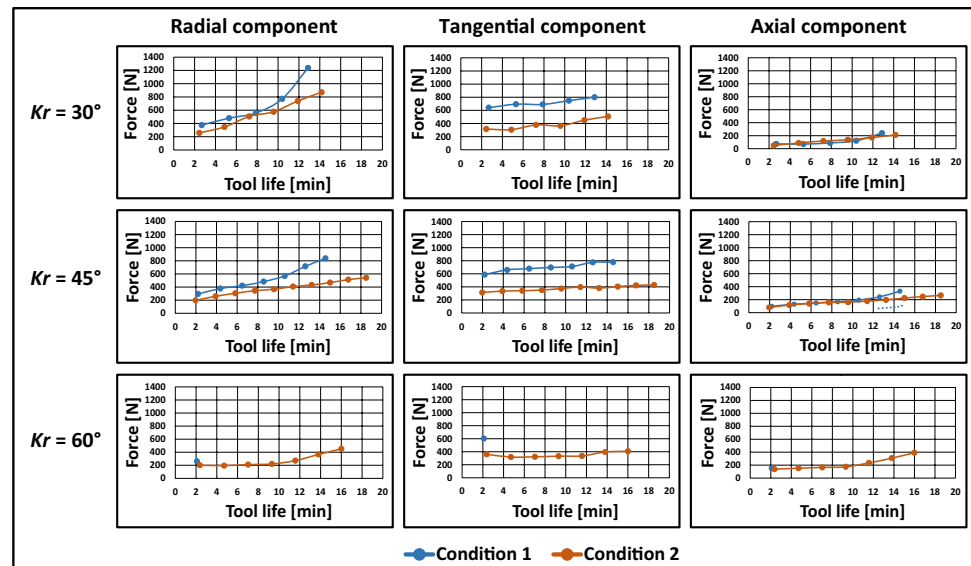
the beginning to 1.11 at the end. The variation is similar at 45° and 60°.

At the beginning (new tool), Fr components are lower than Ft ones since cutting edge is only slightly worn. However, Fr components increase faster than Ft ones, as cutting edge tends to accumulate more and more damage over the flank face. So, at the end of tool life, Fr components are the most significant forces.

If the forces are compared with respect to Kr angle, it can be seen that the forces are higher when low position angles are used.

– Condition 1: the Fr45°/Fr30° ratio varies from 0.79 at the beginning to 0.68 at the end, Ft45°/Ft30° varies from 0.92 at the beginning to 0.97 at the end, and Fa45°/Fa30° varies from 1.35 at the beginning to 1.38 at the end. Regarding the 60° position angle, at the beginning, Fr60°/Fr30° = 0.70, Ft60°/Ft30° = 0.94, and Fa60°/Fa30° = 2.09.
– Condition 2: the Fr45°/Fr30° ratio varies from 0.76 at the beginning to 0.62 at the end, Ft45°/Ft30° varies from 1 at the beginning to 0.84 at the end, and Fa45°/Fa30° varies from 1.62 at the beginning to 1.26 at the end. Secondly, the Fr60°/Fr30° ratio varies from 0.78 at the beginning to 0.52 at the end, Ft60°/Ft30° varies from

1.14 at the beginning to 0.80 at the end, and Fa60°/Fa30° varies from 2.81 at the beginning to 1.86 at the end. The deviations between 30° and 45° angles are very similar to those between 30° and 60°.

Therefore, two important results are derived from the force analysis. The first one is that the Fr component is smaller than the Ft component at the beginning of the machining, but higher at the end. This is true for all three position angles studied, although Fr is more significant at the 30° angle. So, the crossing between both components could be used a control point when it comes replacing the tool. Indeed, in [37], authors observed that radial (passive) component was a good indicator of the evolution of tool wear due to its dramatic increase (in turning of Haynes 282 superalloy). Secondly, force components at 30° are noticeably larger than at the other angles as wear progresses. This is much more pronounced in the case of Fr.

3.4 Surface roughness measurements

Figure 11 shows schematically the variation of the material ridges along the bar as the insert feeds in a single machining step. The height of the ridges is not the same at position 1 as it is at positions 6 or 11, as the effective nose radius decreases due to edge wear.

Fig. 11 Schematic variation of ridge heights
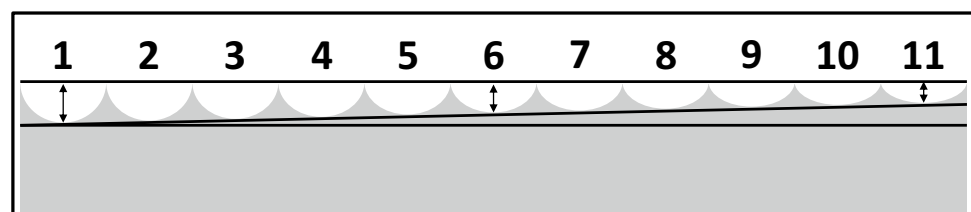
The roughness was measured in the first machining step with a Taylor Hobson® Surtronic Duo roughness meter and the measurement is the average of 3 measurements taken on the surface at the beginning, middle, and end of the bar. In the next machining stage, the average roughness from 3 measurements was obtained. Successive stages were carried out until the insert was broken or worn on the flank. Figure 12 shows, for the different Kr angles and cutting conditions, the evolution of the average, and maximum roughness in each machining step (as an average value of 3 measurements), as well as the corresponding theoretical roughness values. These measurements are compared in the graphs with the theoretical roughness, enunciated by Shaw [38] and which depends on the feed rate and tip radius of the insert ($RZ = f2/(8r\varepsilon)$ y $Ra = RZ/4$).

According to the Shaw equation, low feed rates are advantageous for good surface finish. As can be seen, surface finish in condition 2 tests is significantly better, since the roughness remains around 3–4 μm while the roughness in condition 1 tests remains around 6–7 μm. This result is consistent with the outcome in [14], where the most influential parameter on roughness was feed rate. Although cutting performance of 30°inserts in condition 1 improved safety and offered good performance in terms of the machined volume, surface finish is, in general, worse. So, these cutting conditions can be the best option for rough turning.
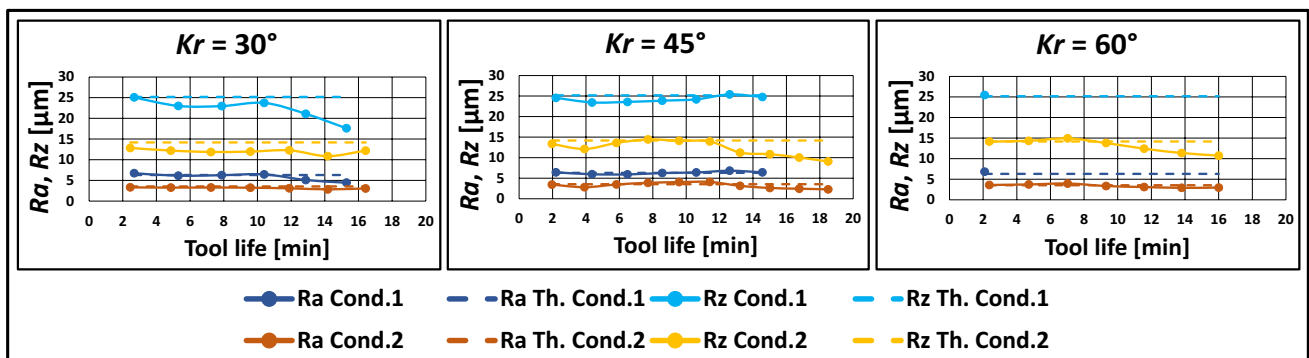

Fig. 12 Surface roughness (Ra and Rz)

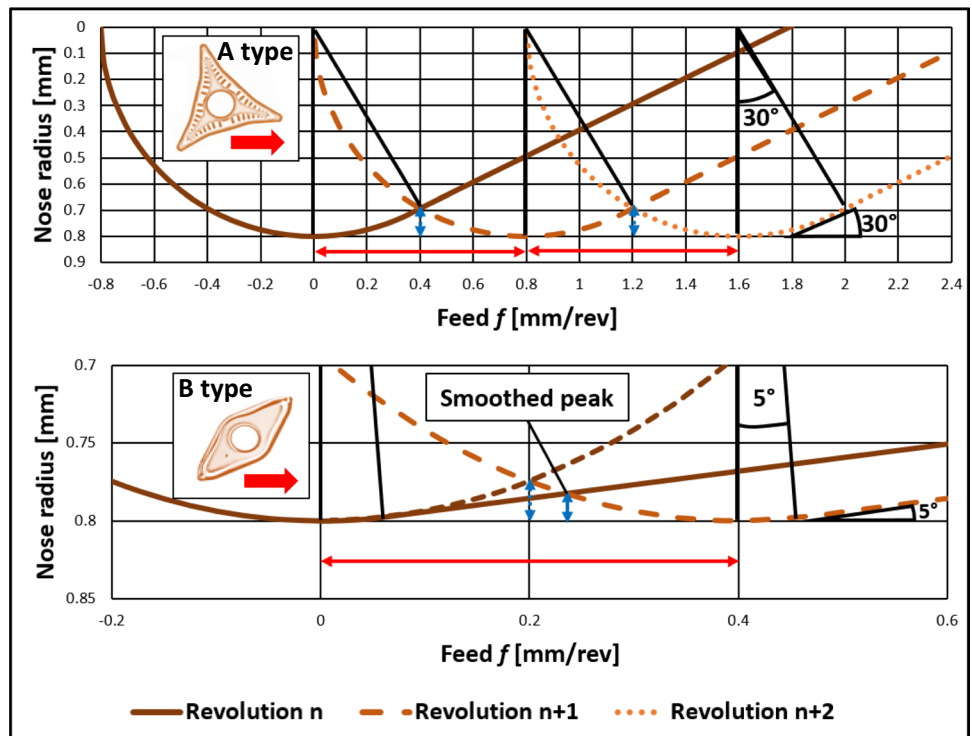**Fig. 13** Roughness profile of types A and B PrimeTurning™ inserts

Figure 13 shows the geometrical analysis of the resulting surface finish for A and B insert-types. At first sight, it seems that a low position angle could decrease the Rz peak roughness. However, a feed higher than 0.8 mm/rev would be necessary for the peak to be lowered on the side of the cutting edge (beyond the nose). As can be seen (Fig. 13), using a wiper edge insert, with a double radius and a very low position angle Kr = 5°, it is possible to smooth the ridges with feeds of 0.3–0.4 mm/rev. This is the case of the PrimeTurning™ insert type B, not used in this work but used by Ráczi et al. [39]. In that work, they observed the roughness Rz obtained with insert type B in roughing does not correlate with the theoretical formulas but with a second order equation (it was found to be about 11 times lower than using the theoretical formula). They also observed that the Rz/Ra ratio does not have a constant value of 4 but is higher (making Ra very low).

Nevertheless, once that wear begins to progress and flatness appears on the insert's nose, the ridges tend to smooth out, slightly reducing surface roughness. In fact, the surface roughness is slightly lower than theoretically expected one, decreasing at the end of the tests.

Specifically for condition 1, − 45°, roughness does not decrease as much, possibly due to a greater presence of built-up edge (BUE) in the intermediate stages (see Table 3). Condition 2, due to its lower feed rate, is clearly better for finishing operations. Besides, at Kr = 30°, despite cutting forces increase, surface finish is improved, as the cutting edge does not suffer breaks or notch wear.

4 Conclusions

PrimeTurning™ is a new technique with promising results when it comes reducing machining times. Especially in the turning of superalloys, it can offer advantages for a more efficient use of tools. However, there are no studies of the behavior of cutting tools under wear conditions and, particularly, a deeper knowledge of the cutting-edge angle is necessary. This work focuses on these two elements—wear and cutting-angle—which are essential to reliably apply this technique in superalloys. To do this, tests were carried out at 2 different cutting conditions: (a) conditions where the effect of chip thickness is dominant (high feed rates and depths of cut) and b) conditions where the thermal effect is more relevant (high cutting speeds). All the tests were repeated using 3 different cutting-edge angles Kr. Cutting forces were monitored, and the integrity of the inserts was inspected. Besides, flank wear and surface roughness were measured at different levels. The following conclusions can be drawn:

– The characteristic wear is a crater wear with BUE and located on the side of the insert when the angle Kr is 30°, but rotated 15° towards the tip when angle Kr is 45° and 30° when angle Kr is 60°, matching the theoretical (geometrical) pattern.
– The simultaneous increase of feed and depth of cut has stronger effects on tool life than cutting speed. Inserts suffering less chip surface removal and higher cutting speed show longer durability, + 7% at Kr = 30°, + 37% at Kr = 45°, and + 65.6% at Kr = 60°.
– Tests with a 30° position angle have shown lower tool life than expected. Long tool-to-workpiece contact times, due to the use of a longer bar and poor chip fractionation, tend to shorten tool life as a result of higher accumulation of heat.
– Results showed that using Kr = 30° reduces the tendency to insert fracture and the likelihood of notches. Chip thickness decreases and the acting force is uniformly spread over a longer edge length. In terms of tool failure, this is the best Kr for the tested conditions.
– High material removal rates lead shorter tool life, but actually perform the best rough levels, in terms of machined volume. Although the risk of tool breakage under these conditions is high, condition 1 with Kr = 30° combines performance and safety against failure, as the tool did not fracture and evacuated 127.7 cm^3 of material compared to 80.1 cm^3 evacuated in finishing conditions.
– Cutting force components are higher using the 30° position angle, especially Fr component which is up to 75% higher than using other Kr angles.
– Forces in PrimeTurning™ are higher in tests with higher ap and f values; a result consistent with the observed edge breaks and shorter tool life.
– The ratio between Fr and Ft components increases throughout the process, especially when Kr = 30°. Here, it varies from 0.57 to 1.49 in condition 1 and from 0.79 to 1.79 in condition 2. This evolution is an indicator of how work material slides on a progressively deforming surface, due to the deterioration of the cutting edge.
– The average and maximum roughness are lower for tests performed at lower feed rates, according to Shaw's equation, so condition 2 is preferable for finishing operations. Besides, roughness is lower as wear progresses, due to its flatness, except when BUE appears. For Kr = 30°, surface quality is improved due to the absence of breaks or notch wear.

Data availability If the paper is accepted, data are not available in repository.

Code availability Not applicable.

Declarations

Ethics approval Not applicable.

Consent for publication Yes.

Conflict of interests The authors declare no competing interests.

References

1. Bushlya V, Schultheiss F, Gutnichenko O, Zhou JM, Stahl J-E (2015) On the analytical representation of chip area and tool geometry when oblique turning with round tools. part 1: chip area parameters under variation of side and back rake angle. Procedia CIRP 31:417–422

2. Urbikain G, Fernández A, de Lacalle LNL, Gutiérrez ME (2013) Stability lobes for general turning operations with slender tools in the tangential direction. Int J Mach Tools Manuf 67:35–44

3. Jiang L, Wang D (2019) Finite-element-analysis of the effect of different wiper tool edge geometries during the hard turning of AISI 4340 steel. Simul Model Pract Theory 94:250–263

4. Fujimaki S, Shibayama T, Hayasaka T, Shamoto E (2020) Proposal of "Curved-profile wiper turning" for efficient, stable, and smooth finishing. Precis Eng 61:152–159

5. Correia AE, Davim JP (2011) Surface roughness measurement in turning carbon steel AISI 1045 using wiper inserts. Measurement 44(5):1000–1005

6. Rahman M, Seah W, Teo TT (1997) The machinability of inconel 718. J Mater Process Technol 63(1–3):199–204

7. Saglam H, Unsacar F, Yaldiz S (2006) Investigation of the effect of rake angle and approaching angle on main cutting force and tool tip temperature. Int J Mach Tools Manuf 46(2):132–141

8. Cascón I, Sarasua JA (2015) Mechanistic model for prediction of cutting forces in turning of non-axisymmetric parts. Procedia CIRP 31:435–440

9. Khan S, Afzal M, Saleem M, Hashmi K, Zakria G (2018) Performance evaluation of novel chamfered inserts in high-feed turning of Ti-6Al-4V alloy. Int J Adv Manuf Technol 97:2319–2329

10. Ráczi V, Sipos S, Farkas G (2018) Chip removal specialities in multi-directional turning. Műszaki Tudományos Közlemények 9(1):207–210

11. Krajčoviech S, Holubjak J, Richtarik M, Czánová T (2021) Identification of process Prime A turning when machining steel C56E2 and monitoring of cutting forces. Transp Res Procedia 55:605–612

12. Amigo FJ, Urbikain G, Pereira O, Fernández-Lucio P, Fernández-Valdivielso A, de Lacalle LNL (2020) Combination of high feed turning with cryogenic cooling on Haynes 263 and Inconel 718 superalloys. J Manuf Process 58:208–222

13. Karpuschewski B, Kundrák J, Varga G, Deszpoth I, Borysenko D (2018) Determination of specific cutting force components and exponents when applying high feed rates. Procedia CIRP 77:30–33

14. Gómez-Escudero G, de Pissón GM, Fernández-Lucio P, Olmo AD, Amigo FJ, Marin F, González H (2022) Nuevos procesos de torneado aplicados a turbinas aeronáuticas, Congreso Iberoamericano de Ingeniería Mecánica-CIBIM, Madrid. http://e-spacio.uned.es/fez/view/bibliuned:congresoCIBIM-2022UPMEspana-Ggomez

15. Zhang X, Wu S, Wang H, Liu C (2011) Predicting the effects of cutting parameters and tool geometry on hard turning process using finite element method. J Manuf Sci Eng 133:041010

16. Reddy RG, Kapoor SG, DeVor RE (1999) A mechanistic force model for contour turning. J Manuf Sci Eng 122(3):398–405

17. Choudhury S, Kishore K (2000) Tool wear measurement in turning using force ratio. Int J Mach Tools Manuf 40(6):899–909

18. Oraby S, Hayhurst D (2004) Tool life determination based on the measurement of wear and tool force ratio variation. Int J Mach Tools Manuf 44(12):1261–1269

19. Zhang G, Guo C (2016) Modeling flank wear progression based on cutting force and energy prediction in turning process. Procedia Manuf 5:536–545

20. Cui X, Li C, Ding W, Chen Y, Mao C, Xu X, Liu B, Wang D, Li HN, Zhang Y, Said Z, Debnath S, Jamil M, Ali HM, Sharma S (2022) Minimum quantity lubrication machining of aeronautical materials using carbon group nanolubricant: From mechanisms to application. Chin J Aeronaut 35(11):85–112

21. Toubhans B, Fromentin G, Viprey F, Karaouni H, Dorlin T (2020) Machinability of inconel 718 during turning: cutting force model considering tool wear, influence on surface integrity. J Mater Process Technol 285:116809

22. Sugihara T, Nishimoto Y, Enomoto T (2017) Development of a novel cubic boron nitride cutting tool with a textured flank face for high-speed machining of Inconel 718. Precis Eng 48:75–82

23. Fernández-Lucio P, Villarón-Osorno I, Neto OP, Ukar E, de Lacalle LNL, del Val AG (2021) Effects of laser-textured on rake face in turning PCD tools for Ti6Al4V. J Market Res 15:177–188

24. Long Y, Huang Y (2010) Combined eefect of flank and crater wear on cutting force modeling in orthogonal machining PART I: MoDevelopment. Mach Sci Technol 14(1):1–23

25. Grechishnikov V, Petukhov Y, Pivkin P, Isaev A, Bushuev S, Romanov V (2015) Prediction and measurement of the parameters of the microtopography of a surface when turning intricately shaped parts. Meas Tech 58:848–853

26. Panda A, Sahoo AK, Rout AK (2016) Investigations on surface quality characteristics with multi-response parametric optimization and correlations. Alex Eng J 55(2):1625–1633

27. Pereira O, Rodríguez A, Fernández-Abia AI, Barreiro J, de Lacalle LNL (2016) Cryogenic and minimum quantity lubrication for an eco-efficiency turning of AISI 304. J Clean Prod 139:440–449

28. Behera BC, Alemayehu H, Ghosh S, Rao PV (2017) A comparative study of recent lubri-coolant strategies for turning of Ni-based superalloy. J Manuf Process 30:541–552

29. Krolczyk GM, Maruda RW, Krolczyk JB, Wojciechowski S, Mia M, Nieslony P, Budzik G (2019) Ecological trends in machining as a key factor in sustainable production – A review. J Clean Prod 218:601–615

30. Khanna N, Agrawal C, Pimenov DY, Singla AK, Machado AR, da Silva LRR, Gupta MK, Sarikaya M, Krolczyk GM (2021) Review on design and development of cryogenic machining setups for heat resistant alloys and composites. J Manuf Process 68:398–422

31. Devillez A, Coz GL, Dominiak S, Dudzinski D (2011) Dry machining of Inconel 718, workpiece surface integrity. J Mater Process Technol 211(10):1590–1598

32. Ibrahim AMM, Omer MAE, Das SR, Li W, Alsoufi MS, Elsheikh A (2022) Evaluating the effect of minimum quantity lubrication during hard turning of AISI D3 steel using vegetable oil enriched with nano-additives. Alex Eng J 61(12):10925–10938

33. Maruda RW, Wojciechowski S, Szczotkarz N, Legutko S, Mia M, Gupta MK, Nieslony P, Krolczyk GM (2021) Metrological analysis of surface quality aspects in minimum quantity cooling lubrication. Measurement 171:108847

34. Gupta MK, Boy M, Korkmaz ME, Yaşar N, Günay M, Krolczyk GM (2022) Measurement and analysis of machining induced tribological characteristics in dual jet minimum quantity lubrication assisted turning of duplex stainless steel. Measurement 187:110353

35. Krolczyk JB, Maruda RW, Krolczyk GM, Wojciechowski S, Gupta MK, Korkmaz ME (2022) Investigations on surface induced tribological characteristics in MQCL assisted machining of duplex stainless steel. J Market Res 18:2754–2769

36. Amigo FJ, Fernández-Valdivielso A, Fernández-Lucio P, Pereira O, Urbikain G, de Lacalle LNL (2022) Influencia del ángulo de posición en el diseño del rompevirutas: estudio de herramientas de torneado dinámico y de alto avance en Inconel® 718, Congreso Iberoamericano de Ingeniería Mecánica-CIBIM, Madrid. http://e-spacio.uned.es/fez/view/bibliuned:congresoCIBIM-2022UPMEspana-Fjamigo

37. Díaz-Álvarez J, Díaz-Álvarez A, Miguélez H, Cantero JL (2018) "Finishing turning of ni superalloy haynes 282". Metals 8:10

38. Shaw MC (1984) Metal Cutting Principles. Oxford University Press, London

39. Ráczi V, Huszák C, Sipos S (2019) High feed turning: roughing and finishing with the same insert? Műszaki Tudományos Közlemények 11:157–160